

Precise quasiparticle energies and Hartree-Fock bands of semiconductors and insulators

Wolfgang von der Linden and Peter Horsch

Max-Planck-Institut für Festkörperforschung, D-7000 Stuttgart 80, Federal Republic of Germany

(Received 8 May 1987)

The GW approximation for the self-energy operator is used to calculate the corrections to band structures obtained within the local-density approximation (LDA). To that end we derive rigorous expressions for the quasiparticle energies and wave functions, being also valid for the exact self-energy. A detailed analysis of the state and energy dependence of the nonlocal exchange-correlation contributions to the quasiparticle energies is given and compared to the approximative self-energies used within the LDA. The self-energy and the dielectric response matrix are evaluated in plane-wave representation. We demonstrate that the wave functions obtained from the empirical pseudopotential model (EPM) are sufficient to compute the final energy bands to within 0.1–0.2 eV. The merit of the EPM wave functions is a fast convergence and the possibility to calculate exchange-correlation self-energies for band structures which are determined in a localized basis. These wave functions incorporate all structural details contained in the *ab initio* wave functions. As far as the dynamics of the dielectric response is concerned a new generalized plasmon-pole concept for the dielectric matrix is introduced which fulfills all important sum rules and possesses the right analytical properties also for the off-diagonal elements. This new scheme provides a significant improvement in computational efficiency. Explicit results are given for germanium.

I. INTRODUCTION

The local-density approximation^{1,2} (LDA) is presently the most successful method for the determination of ground-state properties of solids. The eigenvalues of the LDA equation, though being *a priori* of no physical meaning, are nevertheless commonly interpreted as one-particle energies. The energy gaps obtained thereby are generally much too small. Since the band-structure programs have reached a stage of being well converged it has become clear that this error indicates either a shortcoming of the exchange-correlation (xc) functionals presently used in the LDA or even the principal incapability of the density-functional theory (DFT) to determine excitation energies. Recently it has been shown^{3,4} that the xc potential for the N -particle and the $(N+1)$ -particle system may differ by a finite quantity Δ , often called the discontinuity of the xc functional. As this is a feature even of the “exact” xc functional, the failure of the LDA in describing quasiparticle energies is an intrinsic shortcoming of the (DFT). Godby, Schlüter, and Sham⁵ have demonstrated for several semiconductors that even the exact Kohn-Sham potential leads only to a slight improvement over the LDA results. It has been illustrated by us in a previous paper⁶ for a two-band semiconductor model that every state-independent Kohn-Sham potential $V_{KS}(\mathbf{x})$ is bound to fail in the description of excitation energies because some of the essential physical features are missing.

A possibility to overcome this problem in the framework of the DFT is to determine explicitly the ground-state energies for the N - and the $(N+1)$ -particle system, as proposed recently by Kohn.⁷ This kind of approach, determining excitation energies from total-energy differences, has actually been used before to calculate

many-body corrections to band structures starting out from variational wave functions of the Gutzwiller-Jastrow type.⁸

We will follow here an alternative way to obtain quasiparticle energies using the Green’s-function formalism which allows a direct computation of the exchange-correlation corrections to the LDA band structure. It has been shown recently by *ab initio* and by model calculations^{5,6,9} that the GW approximation (GWA) proposed by Hedin¹⁰ leads to quasiparticle energies in favorable quantitative agreement with experimental data. Its relative simplicity from the point of view of many-body theory enables on the other hand a detailed analysis of the further numerical approximations to be made, such as integration schemes and basis sets.

A further advantage of the Green’s-function scheme is the convenient access to correlation functions. This mediates an understanding of the many-body physics in nearly classical pictures. It is especially the response of the system to an external test charge that provides an interesting insight into the screening behavior of many-body systems and the renormalization of quasiparticles. A detailed discussion of this topic will be the content of a succeeding paper.

In the present paper new techniques for the evaluation of the self-energy in the GWA will be presented. In particular a new generalized plasmon-pole concept has been developed to compute the frequency dependence of the dielectric response matrix. This scheme has the merits that the dielectric matrix always has the correct analytical properties, which is not generally true for the off-diagonal elements in the previous treatment.⁹ Moreover, it implies a faster convergence when calculating the self-energy. We applied the GWA to a series of covalent systems and found a good agreement with experimental re-

sults. The error for the valence-band and the four lowest conduction-band states was always of the order of 0.1 eV. In the present paper we will concentrate on germanium as an example of the high quality of the results obtained by the GWA. Germanium is a particularly challenging case, since the LDA predicts it to be a metal or semimetal^{11,12} (see Fig. 1). We find that the xc corrections to the LDA bands are not simply given by a rigid shift of the conduction bands to higher energies. The deviations from this so-called scissors operator approximation are particularly important in the vicinity of the gap. We observe that the Γ_2 conduction-band state is shifted by 1.02 eV upwards relative to the top of the valence band, whereas at the L point this shift is only 0.73 eV. Subsequently here the xc self-energies decide that Ge is an indirect-gap semiconductor.

Besides the presentation of the quantitative results, the emphasis of the present paper lies on the detailed discussion of the energy and state dependence of the various contributions to the xc functional. This will elucidate also some striking features of the LDA.

A by-product of the GWA is the exchange-only or the Hartree-Fock band structure. Although this approximation yields energy bands for covalent semiconductors that deviate strongly from the exact ones, it is for many reasons important to be able to treat the HFA accurately. First the HF band structure defines the reference energies for the many-body corrections and secondly, for insulators with large energy gaps and weak screening, the exact bands are closer to the HF than to LDA band structure. As has been pointed out before,⁶ the generally very strong cancellations between the nonlocal exchange and the dynamical screening require a very careful treatment of

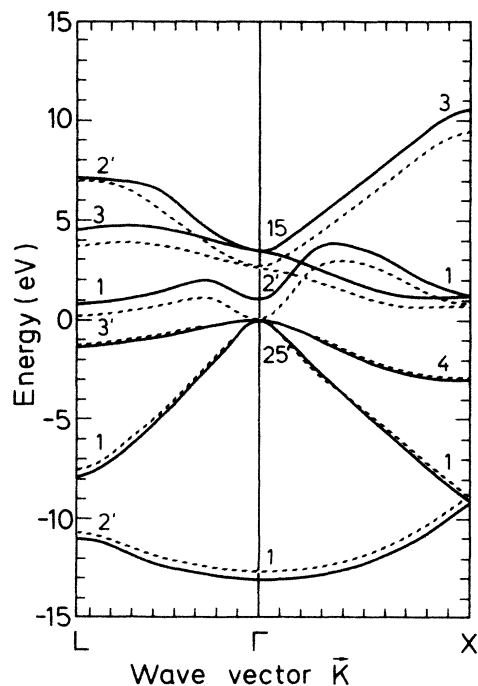


FIG. 1. Band structure of germanium in the LDA (dashed curve, Ref. 11) and the GW approximation (solid curve, present work). The energies are measured in eV.

the nonlocal exchange on the same footing as the correlation. Finally the results for the nonlocal exchange are a well suited test for the accuracy of the computation scheme used for the GWA, since there are recently reliable HFA results available.¹³⁻¹⁷

There have been earlier attempts to obtain the quasiparticle energies of semiconductors by *ab initio* calculations using Green's-function¹⁸ and variational methods.⁸ These investigations provided considerable insight and were actually more sophisticated concerning the treatment of the many-body problem, i.e., in a diagrammatic point of view they went beyond the GW approximation. On the other hand, as only rather small localized basis sets could be handled, their accuracy was limited. In fact much of the present progress has to be attributed to the use of the plane-wave basis which allows for the accurate computation of the nonlocal exchange and dynamical screening within the same framework. This is crucial in view of the strong cancellations. Furthermore the plane-wave basis makes an easy and careful investigation of the convergence possible.

The organization of the paper is as follows. Section II is dedicated to the key ideas leading from the many-body problem in the quasiparticle picture treated in the GWA. In particular we give a rigorous derivation of an expression that allows the perturbative calculation of the quasiparticle wave functions and energies. This provides a tool with which to study the subtle differences between LDA, HFA, and quasiparticle wave functions. This approach may turn out to be of practical importance also for the study of the effect of correlations on defect states. This section furthermore contains the main formulae to be evaluated in the framework of a plane-wave basis.

The dielectric response matrix (DM), for which a new generalized plasmon-pole ansatz for the ω dependence has been developed, is the subject of Sec. III. It will be shown that the concept of the dielectric band structure (DBS) introduced by Baldereschi and Tosatti¹⁹ is a powerful tool in this context. The resulting expressions for the self-energy will be presented in Sec. IV. In the succeeding section a brief discussion follows of the wave functions obtained within the empirical pseudopotential method (EPM) and used for the computation of the self-energy and the dielectric matrix. The resulting HF and finally the correlated quasiparticle band structures, are discussed in Sec. VI and compared to experiment. This section also contains a detailed discussion of the xc contributions to the self-energy, as well as a comparison with the approximations made in the LDA for these quantities. Furthermore, a discussion of previous work will be presented here. This section can be read independently of the others so that the reader only interested in the final results and discussions may go directly to it. The key points of this paper are summarized in Sec. VII together with an outlook on further applications. The Appendices A-C contain details concerning the calculation of the exact quasiparticle wave functions, the generalized f sum rule and some implications for the treatment of the dielectric response, and finally the scheme of how the Brillouin-zone integrations over singular integrands are performed.

II. GW APPROXIMATION

The Green's-function formalism¹⁰ is a very convenient tool for the computation of quasiparticle quantities since it directly gives the response of the N -particle system when an electron is added to or subtracted from the system.

The N -electron Schrödinger equation reduces in the framework of the Green's-function formalism via Dyson's equation to a quasiparticle equation:

$$h_0(\mathbf{x})\Phi_\mu(\mathbf{x}) + \int d^3\mathbf{x}' \Sigma^{\text{xc}}(\mathbf{x}, \mathbf{x}'; \varepsilon_\mu) \Phi_\mu(\mathbf{x}') = \varepsilon_\mu \Phi_\mu(\mathbf{x}). \quad (1)$$

Here μ includes both the band index as well as the wave vector. The quasiparticle states $\Phi_\mu(\mathbf{x})$ form a complete set of functions but they are in general neither normalized nor linear independent. Due to the nonhermiticity of the Hamiltonian the quasiparticle energies ε_μ are in general complex. The real part corresponds to the excitation energy and the imaginary part is related to the finite lifetime of the quasiparticle. The Hartree Hamiltonian $h_0(\mathbf{x})$ contains the contributions of the kinetic energy, the electron-ion interaction, and the Hartree potential. Σ^{xc} represents the nonlocal and energy-dependent self-energy operator which is related via a coupled set of integral equations¹⁰ to the one-electron Green's function:

$$G(\mathbf{x}, \mathbf{x}'; \omega) = \sum_\mu \frac{\Phi_\mu(\mathbf{x})\Phi_\mu^*(\mathbf{x}')}{\omega - \varepsilon_\mu - i\delta^+ \text{sgn}(\varepsilon_F - \varepsilon_\mu)}, \quad (2)$$

to the *screened Coulomb interaction*

$$\varepsilon(\mathbf{x}, \mathbf{x}'; \omega) = \delta(\mathbf{x} - \mathbf{x}') + \frac{1}{2\pi i} \int d^3\mathbf{y} v(\mathbf{x} - \mathbf{y}) \int d\omega' e^{i0^+ \omega'} G(\mathbf{y}, \mathbf{x}'; \omega - \omega') G(\mathbf{x}', \mathbf{y}; \omega'). \quad (6)$$

In the GWA all quantities are completely determined by the one-electron Green's function. For completeness we also note the formula for the ground-state density

$$n(\mathbf{x}) = \frac{1}{2\pi i} \int d\omega' e^{i0^+ \omega'} G(\mathbf{x}, \mathbf{x}; \omega') = \sum_\mu n_\mu |\Phi_\mu(\mathbf{x})|^2. \quad (7)$$

In the interacting ground state the *occupation number* n_μ is in general not a simple step function. The GWA forms a coupled set of equations. For a given starting potential, Σ_0^{xc} , Eq. (1) provides a set of wave functions and energies which then define an improved self-energy and so forth. A well-suited starting potential Σ_0^{xc} is supplied by the LDA as the ground-state density is well described. The quasiparticle description in the framework of the Green's-function formalism *a posteriori* justifies the interpretation of the eigenvalues $\varepsilon_\mu^{\text{KS}}$ and eigenvectors $|\Phi_\mu^{\text{KS}}\rangle$ of the Kohn-Sham equation as approximate quasiparticle quantities, which is not obvious from the DFT point of view.^{1,2} The LDA xc potential being local and state independent [$\Sigma_{\text{LDA}}^{\text{xc}}(\mathbf{x}, \mathbf{x}'; \omega) = \delta(\mathbf{x} - \mathbf{x}') V_{\text{LDA}}^{\text{xc}}(\mathbf{x})$] supplies a Hermitian Hamiltonian and hence real energies, orthogonal wave functions, and a step function for the occupation numbers $n_\mu = \Theta(\varepsilon_F - \varepsilon_\mu)$. Once the LDA one-

$$W(\mathbf{x}, \mathbf{x}'; \omega) = \int d^3\mathbf{y} v(\mathbf{y}) \varepsilon^{-1}(\mathbf{x} - \mathbf{y}, \mathbf{x}'; \omega), \quad (3)$$

and to the vertex function

$$\Gamma = 1 + \frac{\delta\Sigma}{\delta V}. \quad (4)$$

In the above equation ε_F stands for the Fermi energy, v denotes the bare Coulomb interaction, and ε^{-1} is the inverse dielectric matrix defined below. The GWA consists of neglecting vertex corrections, or in other words, Γ is equated to 1. This corresponds to the first-order term in the series expansion of the self-energy with respect to the *screened interaction* W . In this approximation the expression for the self-energy reads

$$\Sigma^{\text{xc}}(\mathbf{x}, \mathbf{x}'; \omega) = \frac{1}{2\pi i} \int d\omega' e^{i0^+ \omega'} G(\mathbf{x}, \mathbf{x}'; \omega - \omega') \times W(\mathbf{x}, \mathbf{x}'; \omega'), \quad (5)$$

with 0^+ being an infinitesimal small positive number.

It has been argued by Hedin and Lundqvist¹⁰ that vertex corrections for the self-energy are negligible for the homogeneous electron gas. To our knowledge there is only the work by Minnhagen²⁰ in which the vertex corrections have been analyzed in more detail. Despite some analyticity problems, the results nevertheless indicate the unimportance of vertex corrections to the quasiparticle energies. Indirectly this statement is supported by the promising results achieved so far by the GWA.^{5,6,9} The same approximation for the dielectric function leads to the random-phase-approximation (RPA) formula

particle quantities are known, there is a convenient way to determine the exact quasiparticle energies $\varepsilon_\mu^{\text{ex}}$ and wave functions $|\Phi_\mu^{\text{ex}}\rangle$:

$$\Delta\varepsilon_\mu = \varepsilon_\mu^{\text{ex}} - \varepsilon_\mu^{\text{KS}} = \langle \Phi_\mu^{\text{KS}} | \Delta\Sigma^{\text{xc}}(\varepsilon_\mu^{\text{ex}}) | \Phi_\mu^{\text{ex}} \rangle, \quad (8a)$$

$$|\Phi_\mu^{\text{ex}}\rangle = \frac{1}{1 - P_\mu G^0(\varepsilon_\mu^{\text{ex}}) \Delta\Sigma^{\text{xc}}(\varepsilon_\mu^{\text{ex}})} |\Phi_\mu^{\text{KS}}\rangle. \quad (8b)$$

Here the projection operator $P_\mu = 1 - |\Phi_\mu^{\text{KS}}\rangle \langle \Phi_\mu^{\text{KS}}|$ and the Green's function $G^0(\omega)$ are defined with respect to the eigenfunctions of the Kohn-Sham Hamiltonian. The last unknown entity in Eq. (8) is the residual self-energy:

$$\Delta\Sigma^{\text{xc}}(\omega) = \Sigma^{\text{xc}}(\omega) - \Sigma_{\text{KS}}^{\text{xc}}. \quad (8c)$$

In the above equation abundant indices have been dropped. For more details concerning Eq. (8) see Appendix A. A similar expression for the energy correction to the Kohn-Sham band gap has been derived by Sham and Schlüter.⁴ Their formula has been criticized by Gunnarsson and Schönhammer.²¹ The main difference of our result to that of Ref. 4 lies in the projection operator and the exact quasiparticle energies instead of the Kohn-Sham energies in the arguments.²² The higher-order

corrections to the quasiparticle energies are determined by the changes of the quasiparticle wave functions. It is instructive to consider the two-band model.⁶ In this case the gap is opened by the pseudopotential which already determines the precise form of the wave functions at the gap. Exchange-correlation corrections affect the size of the gap but do not lead to further changes in the wave functions. Therefore the first-order term already gives the exact result.

III. DIELECTRIC RESPONSE MATRIX

In this section we turn to the dielectric matrix (DM) which determines the screened interaction W . We applied the random-phase approximation which is reminiscent of the GWA for the self-energy as it is the first term of an expansion with respect to W .

Our calculations have been performed in a plane-wave basis using the Adler-Wiser formalism^{23–25} for the *Hermitian* dielectric matrix:

$$\begin{aligned} \epsilon_{\mathbf{G},\mathbf{G}'}(\mathbf{q};\omega) &= \delta_{\mathbf{G},\mathbf{G}'} + \frac{4\pi}{\|\mathbf{q}+\mathbf{G}\| \|\mathbf{q}+\mathbf{G}'\|} \alpha_{\mathbf{G},\mathbf{G}'}^0(\mathbf{q};\omega), \\ \alpha_{\mathbf{G},\mathbf{G}'}^0(\mathbf{q};\omega) &= 2 \sum_{\mathbf{k}} \sum_{n,m} f_n (1-f_m) \frac{\rho_{\mathbf{k},\mathbf{q}}(\mathbf{G}) \rho_{\mathbf{k},\mathbf{q}}^*(\mathbf{G}')}{\omega - [\epsilon_n(\mathbf{k}) - \epsilon_m(\mathbf{k}+\mathbf{q})]}, \end{aligned} \quad (9)$$

$$\rho_{\mathbf{k},\mathbf{q}}(\mathbf{G}) = \langle \mathbf{k}, n | e^{i(\mathbf{q}+\mathbf{G})\cdot\mathbf{x}} | \mathbf{k}+\mathbf{q}, m \rangle.$$

For the Brillouin-zone integration the Chadi-Cohen scheme²⁶ with ten special points has been employed.

To perform the ω integration for the self-energy [Eq. (5)] analytically it is convenient to introduce a generalized plasmon-pole ansatz for the frequency dependence of the DM. Alternatively the ω integration can be performed numerically along the imaginary axis, as it has been done by Godby *et al.*⁵ We preferred the former scheme since it is computationally less expensive. The final results are the same in both cases.

We express the static DM in its eigenrepresentation:

$$\epsilon_{\mathbf{G},\mathbf{G}'}^{-1}(\mathbf{q};0) = \delta_{\mathbf{G},\mathbf{G}'} + \sum_{i=1}^{\infty} U_{\mathbf{q},i}(\mathbf{G}) [\epsilon_i^{-1}(\mathbf{q}) - 1] U_{\mathbf{q},i}^*(\mathbf{G}'). \quad (10)$$

Here U is the matrix formed by the eigenvectors of the inverse dielectric matrix. The discussion of dielectric properties in terms of the dielectric band structure (DBS), i.e., in terms of the eigenvalues $\epsilon_i^{-1}(q)$ of the DM, has been introduced by Baldereschi and Tosatti.¹⁹

In order to obtain the generalized plasmon-pole approximation it is natural to introduce the frequency dependence in the eigenvalues, i.e.,

$$\epsilon_i^{-1}(q,\omega) - 1 = \frac{z_i(\mathbf{q})}{\omega^2 - [\omega_i(\mathbf{q}) - i\delta]^2}. \quad (11)$$

For $\omega=0$ this equation provides a relationship between the dielectric band structure, the unknown pole strength $z_i(\mathbf{q})$, and the plasmon dispersion $\omega_i(\mathbf{q})$. The second relationship which determines these quantities uniquely is given by the Johnson sum rule (Appendix B). This results in

$$\begin{aligned} z_i(\mathbf{q}) &= \frac{\omega_{\text{pl}}^2}{\rho(0)} \sum_{\mathbf{G},\mathbf{G}'} U_{\mathbf{q},i}^*(\mathbf{G}) \frac{(\mathbf{q}+\mathbf{G})\cdot(\mathbf{q}+\mathbf{G}')}{\|\mathbf{q}+\mathbf{G}\| \|\mathbf{q}+\mathbf{G}'\|} \\ &\quad \times \rho(\mathbf{G}-\mathbf{G}') U_{\mathbf{q},i}(\mathbf{G}'), \end{aligned} \quad (12)$$

and

$$\omega_i^2(\mathbf{q}) = \frac{z_i(\mathbf{q})}{1 - \epsilon_i^{-1}(\mathbf{q})}. \quad (13)$$

Here Eq. (12) contains the free-electron plasma frequency $\omega_{\text{pl}}^2 = 4\pi\rho(0)$ and the Fourier transform of the ground-state density $\rho(\mathbf{G})$.

The pole strength can also be expressed in terms of the real-space eigenpotentials $\Psi_{\mathbf{q},i}(\mathbf{x})$ of the DM,^{19,27} which are defined in Appendix B:

$$z_i(\mathbf{q}) = \frac{\omega_{\text{pl}}^2}{\rho(0)} \int d^3\mathbf{x} \rho(\mathbf{x}) \|\nabla_{\mathbf{x}} \Psi_{\mathbf{q},i}(\mathbf{x})\|^2. \quad (14)$$

In this representation the magnitude of the pole strength can easily be discussed. One immediately realizes that it is positive definite. Furthermore, it is proportional to the overlap between the ground-state density and the eigenfields of the DM to the quantum number (\mathbf{q}, i) which drops rapidly with increasing i . The eigenvalues $\epsilon_i^{-1}(\mathbf{q})$ of the static dielectric matrix in the RPA lie in the interval $(0,1)$.²⁷ Consequently, the plasmon frequencies (12) are all real, contrary to the approach suggested by Hybertsen and Louie.²⁸

Concerning a detailed discussion of this ansatz for the dynamics of the DM and other features of the dielectric response to a quasiparticle we refer to a succeeding publication. Here we just mention that the off-diagonal elements lose their pole structure with increasing distance from the diagonal. This is reflected in the DBS plasmon-pole ansatz in an increasing number of poles that contribute effectively to these elements. Allowing for a small broadening of the plasmon poles leads to an almost complete agreement with the ω dependence of the directly calculated matrix elements.

IV. THE SELF-ENERGY

The DBS plasmon-pole ansatz leads to the following expressions for the numerical evaluation of the matrix elements of the self-energy operator in the basis of the LDA wave functions:

$$\langle \Phi_{\mathbf{p},n_0}^{\text{LDA}} | \Sigma^{\text{corr}}(\omega) | \Phi_{\mathbf{p},n_0}^{\text{LDA}} \rangle = \frac{1}{2} \sum_{n=1}^{\infty} \frac{1}{V} \sum_{\mathbf{q}} \sum_{i=1}^{\infty} \frac{z_i(\mathbf{q}) [S_{\mathbf{q},n}^{\mathbf{p},n_0}(i)]^* S_{\mathbf{q},n}^{\mathbf{p},n_0}(i)}{\omega_i(\mathbf{q}) [\omega - \epsilon_{\mathbf{p}-\mathbf{q},n} + \text{sgn}(\epsilon_F - \epsilon_{\mathbf{p}-\mathbf{q},n}) \omega_i(\mathbf{q})]}, \quad (15a)$$

where the generalized overlap matrix is defined as

$$S_{q,n}^{p,n_0}(i) = \int d^3\mathbf{x} \Phi_{p,n_0}^*(\mathbf{x}) \Psi_{q,i}(\mathbf{x}) \Phi_{p-q,n}(\mathbf{x}). \quad (15b)$$

The Ψ 's are, as before, the real-space eigenpotentials of the DM. The first sum in Eq. (15a) runs over all quasiparticle band indices in the first Brillouin zone (1BZ), while the i summation goes over the dielectric bands. This sum converges rapidly due to the generalized overlap matrix S . In the generalized plasmon-pole approximation of Ref. 9 a summation over the reciprocal-lattice vectors appears instead which exhibits a slower convergence. A further crucial point is the factorization in the indices n_0, n'_0 which allows the computation of the full self-energy matrix in the same amount of time that is needed for the diagonal elements. This is important if the wave functions have to be updated. We performed our calculation within a plane-wave basis in which the quasiparticle wave functions are

$$\Phi_{p,n}(\mathbf{x}) = \frac{1}{\sqrt{V}} \sum_{\mathbf{G}} \Phi_{p,n}(\mathbf{G}) e^{i(\mathbf{p}+\mathbf{G})\cdot\mathbf{x}}. \quad (16)$$

The corresponding expression holds for the eigenpotentials.

This transforms the generalized overlap matrix S of Eq. (15) into

$$S_{q,n}^{p,n_0}(i) = \sum_{\mathbf{G}, \mathbf{G}'} \Phi_{p,n_0}^*(\mathbf{G}) \Psi_{q,i}(\mathbf{G}-\mathbf{G}') \Phi_{p-q}(\mathbf{G}'). \quad (17)$$

Note that the eigenpotentials Ψ for the non-Hermitian dielectric matrix are related to the eigenpotentials U of the Hermitian dielectric matrix of Eq. (11) via $\Psi_{p,i}(\mathbf{G}) = [v(\mathbf{p}+\mathbf{G})]^{1/2} U_{q,i}(\mathbf{G})$, where $v(\mathbf{q}) = 4\pi/q^2$ is the Fourier transform of the bare Coulomb interaction.²⁷

So far we have only discussed the correlation contribution to the self-energy. In contrast to the complicated standard HF scheme, the matrix elements for the nonlocal exchange take here the strikingly simple form

$$\begin{aligned} \langle \Phi_{p,n_0}^{\text{LDA}} | \Sigma^x | \Phi_{p,n_0}^{\text{LDA}} \rangle &= -\frac{1}{V} \sum_{\mathbf{q}} \sum_n \sum_{\mathbf{G}} v(\mathbf{p}-\mathbf{q}+\mathbf{G}) \\ &\quad \times [C_{q,n}^{p,n_0}(\mathbf{G})]^* \\ &\quad \times C_{q,n}^{p,n'_0}(\mathbf{G}), \end{aligned} \quad (18a)$$

with

$$C_{q,n}^{p,n_0}(\mathbf{G}) = \sum_{\mathbf{G}'} \Phi_{p,n_0}^*(\mathbf{G}+\mathbf{G}') \Phi_{q,n}(\mathbf{G}'). \quad (18b)$$

In the expression for the residual self-energy of Eq. (8c) the matrix elements of the LDA xc potential have to be subtracted from the GWA results.

In the basis of the LDA wave functions the transformation matrix entering into Eq. (8b) is given by

$$\begin{aligned} [1 - P_{p,m} G^0(\epsilon_{p,m}) \Delta \Sigma^{\text{xc}}]_{p,n;p,n'} \\ = \delta_{n,n'} - \frac{(1 - \delta_{n,m}) \Delta \Sigma_{p,n;p,n'}^{\text{xc}}}{\epsilon_{p,m} - \epsilon_{p,n}^{\text{LDA}}}. \end{aligned} \quad (19)$$

The inverse of this matrix determines, according to Eq. (8b), the exact quasiparticle states for wave vector \mathbf{p} and band index m . Clearly the transformation from LDA to the exact states does not mix different \mathbf{p} vectors. For unperturbed crystals the transformation matrix is to a good approximation the unit matrix as has been found by Hybertsen and Louie.⁹ The deviations from LDA wave functions will come into play for impurities and surfaces, for which Eqs. (8) and (19) could provide a convenient tool to compute the correct wave functions.

For our purpose it is sufficient to take the LDA wave functions. In that case the energy corrections are just the diagonal part of Eq. (15).

V. SINGLE-PARTICLE WAVE FUNCTIONS

In the self-consistent solution the exchange-correlation self-energy and the dielectric matrix are finally determined by the exact quasiparticle wave functions and energies [Eq. (8)]. The LDA already provides a very good starting set for these quantities, which may be computed, e.g., by an *ab initio* pseudopotential calculation using a plane-wave representation.

Instead, we shall use here empirical pseudopotential wave functions,²⁹⁻³³ which already contain all the structural details of the *ab initio* wave functions. The empirical pseudopotential method (EPM) has been a remarkably important tool for the evaluation of the dielectric matrix,^{24,25} supplying very accurate results. The similarity of the expressions for the DM and those for the self-energy suggests to make use of the EPM also for that purpose.

An additional feature of the EPM is the restriction to very few reciprocal-lattice vectors in the expansion of the pseudopotentials, namely three potential parameters for homopolar semiconductors and six parameters for ionic systems. Nevertheless the expansion of the wave function in plane waves must be extended to a much larger number of reciprocal-lattice vectors. In our calculation it turned out that 89 plane waves are sufficient for the precise calculation of the self-energy.

The potential form factors characterizing the EPM bands and wave functions are determined such that the experimental band structure is reproduced.³¹ Alternatively one can also choose form factors which represent the LDA band structure. In this case one has to add the self-energy correction to the LDA energy to obtain a first approximation to the quasiparticle energy. After a few iteration steps convergence is achieved. The final result is the same within the present accuracy of 0.1 eV in both cases.

This scheme has the particular advantage that one is in the position to compute also exchange-correlation corrections to LDA band structures determined in a localized basis, e.g., Gaussians or linearized muffin-tin orbitals (LMTO's).

We want to stress here that the EPM is more than a very efficient method to represent energy bands; it also provides a good approximation to the wave functions and densities. In Fig. 2 we give an example for the rather dramatic state dependence of the Bloch functions, or more precisely of their partial densities $|\Phi_{\mathbf{k},n}(\mathbf{x})|^2$.

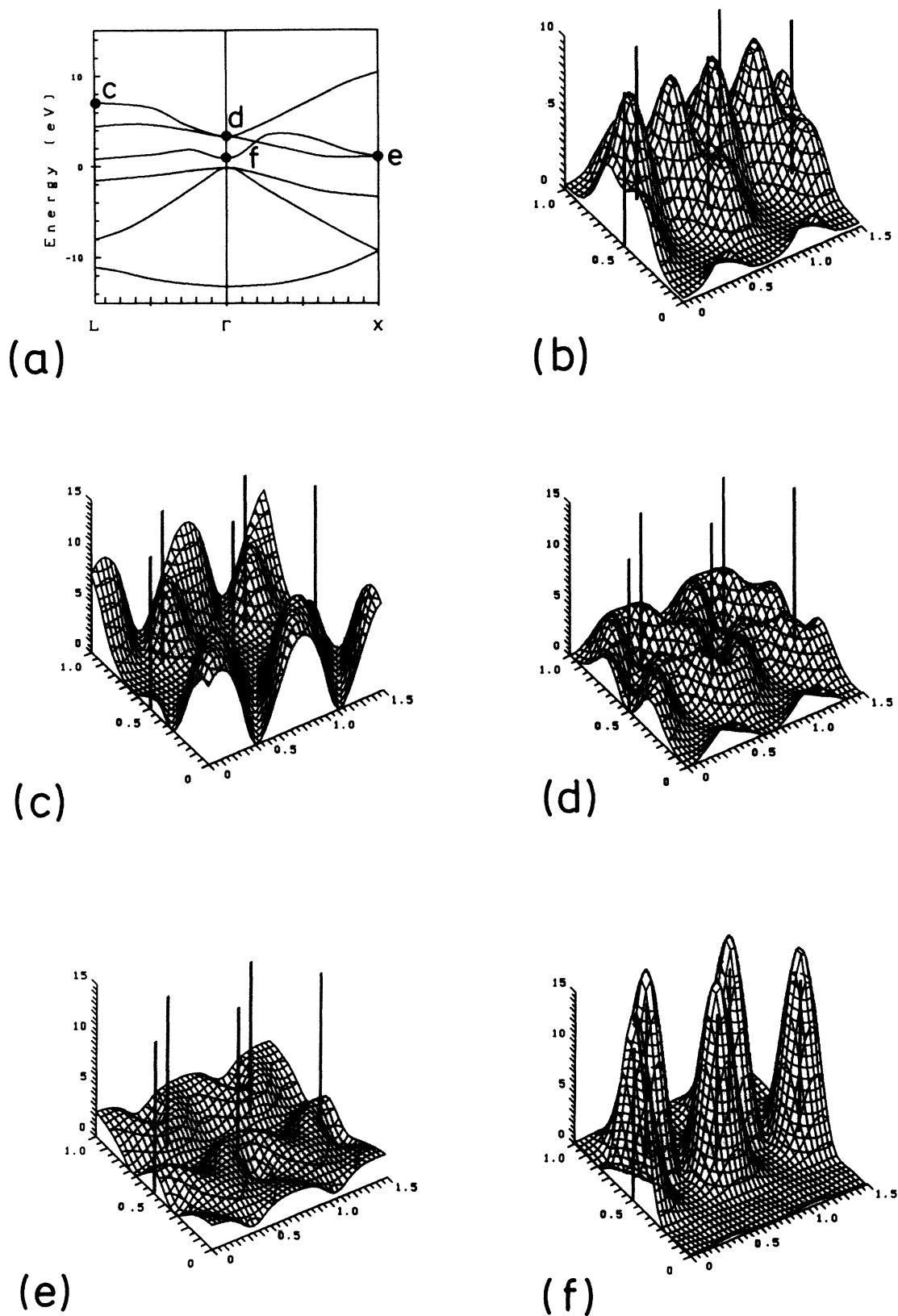


FIG. 2. Partial densities $|\Phi_{k,n}(\mathbf{x})|^2$ for selected Bloch states. The labels in the band structure of Ge (a) indicate the particular states (c)–(f) displayed, and (b) gives the ground-state density. The $(1\bar{1}0)$ plane shown contains a zigzag chain of atoms with positions indicated by vertical bars. The axes in the plane are in $[110]$ and $[001]$ directions. The densities are given in atomic units.

Since these changes are very pronounced, even within one band, one would tend to presume that this state dependence should turn out also in the exchange-correlation energy. The selected states, shown in Figs. 2(c)–2(f), correspond to band-structure points as indicated in Fig. 2(a). For comparison, the total ground-state density, reflecting the typical covalent bonds, is plotted in Fig. 2(b). The states in Figs. 2(c)–2(f) belong to the four lowest conduction bands. The highest state at the L point has all its weight in the interstitial region while the lowest state at the Γ point, which is of antibonding s -orbital character, is strongly localized at the atomic positions. The threefold-degenerate Γ_{15} state shows the density distribution of an antibonding p orbital. The lowest X -point state has its highest density in the interstitial regions. It has been proposed in the case of silicon³⁴ to make use of this special feature of the wave function to tune the gap by shifting the lowest conduction-band state via changes of the potentials in the interstitial regions.

This brings us to the central question as to what extent these large differences of the single-particle states are reflected in the nonlocal and energy-dependent exchange-correlation self-energy. This question is particularly interesting in view of the local and state-independent potential used in the LDA. In the following section we will analyze in detail the state dependence of the self-energy arising from the nonlocal exchange, the local exchange which enters the LDA equations, as well as the energy-dependent correlation contributions.

VI. RESULTS

We start with the discussion of the HF band structure. There have been numerous attempts to calculate HF bands for semiconductors; nevertheless, solving these self-consistent equations still remains a difficult problem and no really superior method turned out. On the other hand progress has been made by realizing that the wave functions obtained by an LDA calculation are close to the HF-wave functions and can actually replace them in the computation of HF ground-state energies and energy bands.¹⁴ Thereby the problem of iterating the HF equations to convergence is avoided.

The nonlocal exchange forms the largest contribution to the self-energy and its precise calculation is crucial for any reliable determination of correlated band structures. Of course the nonlocal exchange is counteracted by screening, thereby reducing its effect depending on the size of the polarizability of the material. The only other HF calculation for germanium is, to our knowledge, that of Svane,¹⁷ employing the LMTO tight-binding technique.^{35,36} In the HFA we find for the gap and the valence-band width 4.9 and 18.2 eV, respectively. A comparison of our HF band structure, derived from the LDA bands of Bachelet and Christensen,¹¹ and that of Svane shows remarkable agreement (Fig. 3). This is more surprising in view of the completely different characters of the basis sets employed in these calculations. The remaining small discrepancy localized mainly in the vicinity of the $\Gamma_{25'}$ point is partially related to the more accurate integration scheme used here (see Appendix C).

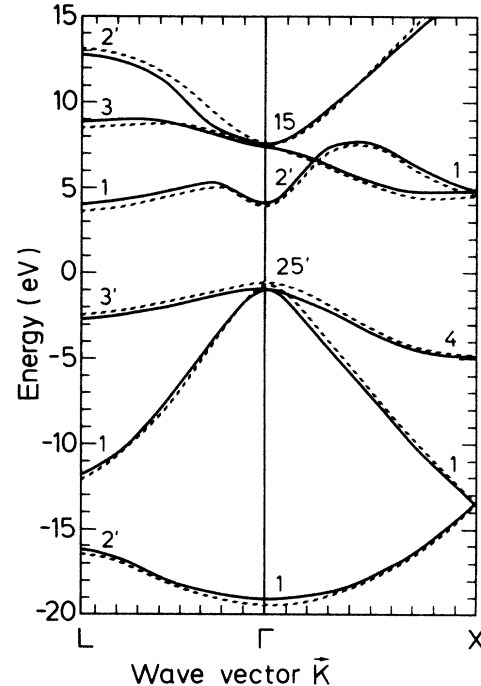


FIG. 3. Hartree-Fock band structure of germanium in eV. The solid curve represents the result of the present work for a plane-wave basis, while the dashed curve is the result of the tight-binding LMTO scheme (Ref. 17).

An instructive way to analyze the self-energy corrections is to plot them versus the LDA energies of the individual states. The resulting function is not unique as in general there exist several quantum numbers (k, n) corresponding to the same LDA energy, which will not necessarily have the same exchange energy.

The result for the nonlocal exchange is given in Fig. 4(a). The main feature of the exchange correction can be characterized by an average smooth curve, namely by one straight line for the valence bands and one, possessing a different slope, for the conduction band. Both curves are separated by a gap of about 7 eV. In addition the result exhibits “fluctuations” around these mean curves which arise from the anisotropy of the system, the different symmetries of the wave functions, and their different locations within the unit cell. Henceforth we will call these briefly anisotropy effects. The most dominant anisotropy effects are found for states which are well localized in the interstitial regions. It is clear that they have smaller exchange energy due to the smaller overlap between these states and the valence wave functions.

We proceed with the discussion of the local approximation for the exchange. The lower set of points in Fig. 4(b) shows an analogous plot for the local exchange as it enters into the LDA ($V_{\text{LDA}}^x = [3\rho(\mathbf{x})/\pi]^{1/3}$). At first glance these data seem to have nothing in common with the nonlocal exchange. The main effect of the local exchange is merely to shift all the energy bands by roughly $-k_F/\pi$, which is the value for the homogeneous electron gas at the Fermi momentum k_F . Hence the pronounced state dependence of the nonlocal exchange also present in

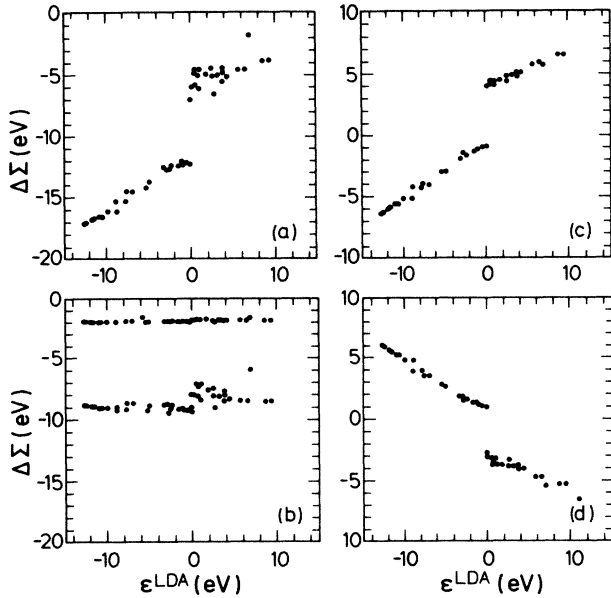


FIG. 4. Plot of different self-energy contributions for a large number of states vs their LDA energies: (a) nonlocal exchange, (b) local exchange (lower set of points) and correlation contribution in the LDA (upper set of points), (c) difference between nonlocal and local exchange, and (d) correlation self-energy calculated in the *GW* approximation.

the homogeneous electron gas¹⁰ is discarded in the local approximation. It is this state dependence that is responsible for the large HF gaps. This can be easily understood in terms of a two-band model.^{6,37} Figure 4(b) immediately explains why the LDA bandwidths and gaps are generally much smaller than in the HF approximation. The local exchange increases the gap by about 1 eV in contrast to about 7 eV the nonlocal exchange brings about. In addition to the overall state dependence, we recognize pronounced “fluctuations” that stem from the \mathbf{x} dependence of $V_{\text{LDA}}^x(\mathbf{x})$ and as the most startling result we find that these fluctuations are almost the same as they appear in the nonlocal exchange. Subtracting the results of the local from those of the nonlocal exchange one obtains the smooth curve of Fig. 4(c) with only minor fluctuations. This observation actually corroborates the assumptions made for the two-band model.^{6,37}

Figure 4(d) exhibits the detailed results for the correlation correction. We observe that the fluctuations in the correlation self-energy are much smaller than in the data for the exchange. For comparison also the correlation self-energy used in the LDA is given in Fig. 4(b). For V_c^{LDA} we have chosen the RPA expression supplied by the homogeneous electron gas which corresponds to the *GW* approximation. The contribution of V_c^{LDA} to the gap is vanishingly small. It is solely a rigid downward shift of about 1.9 eV for all bands which lowers the total energy but does not affect the shapes and relative positions of the bands. The total xc correction, namely $\Delta\Sigma^{\text{xc}} = \Sigma_{\text{exact}}^{\text{xc}} - \Sigma_{\text{LDA}}^{\text{xc}}$, is plotted in Fig. 5. As expected, the screening strongly reduces the exchange correction, leading to a final result reminiscent of a disfigured scissors operator

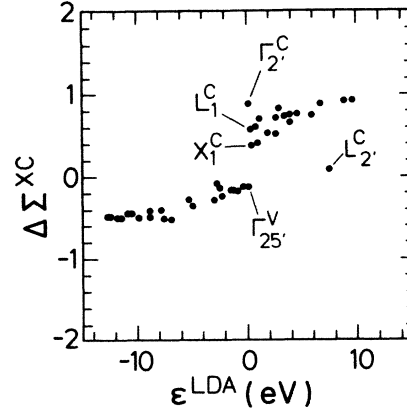


FIG. 5. Total xc self-energy $\Delta\Sigma^{\text{xc}}$ computed in the *GWA* plotted vs the LDA energy of these states.

with a discontinuity of about 1 eV. Yet the deviations from the simple step function in the vicinity of the gap are important as to the correct topology of the conduction band. Whereas in the LDA the lowest conduction-band states at L and Γ are almost degenerate, it is the difference in the xc corrections of 0.73 eV at L and 1.02 eV at Γ which determines Ge to be an indirect-gap semiconductor (Table I). For the indirect gap we find 0.82 eV when starting from the LDA calculation of Bachelet and Christensen¹¹ and 0.67 eV when using the more recent LDA results of Christensen;¹² this has to be compared to the experimental gap of 0.74 eV.

A particularly large deviation from the scissors operator is found for the highest conduction-band state at L (Table I). The $L_{\frac{1}{2}}^c$ state has a very high amplitude in the interstitial region, see Fig. 2(c). The two LDA calculations differ here somewhat, while their agreement is otherwise almost perfect. This excellent agreement between LDA calculations based on LMTO's and on plane waves, respectively, has been pointed out recently by Bachelet and Christensen.¹¹ In view of our xc corrections we find good agreement with experiment for this particular state if we adopt the figure quoted by Christensen¹² (Table I). A comparison of the LDA and the *GW* band structure is given in Fig. 1.

The correlation correction to the gap can roughly be described⁶ by $\Delta\Sigma^c \approx -\Delta\Sigma^x(1-1/\epsilon_0)$. This formula reflects the decisive trend that the HFA becomes a good approximation for large gap insulators ($\epsilon_0 \rightarrow 1$), while in the case of small gaps ($\epsilon_0 \gg 1$) the LDA is more reliable. This expression for $\Delta\Sigma^c$ also explains why the RPA dielectric matrix already gives quite accurate results for the band structure, although the macroscopic dielectric constant ϵ_M calculated in the RPA is generally about 10% too small. For germanium $\epsilon_M^{\text{RPA}} = 14.5$ compared to the experimental value of 16.0. This leads, however, to a change of $1-1/\epsilon_0$ of 0.7% or to an error in the gap of about 0.03 eV. This uncertainty is an order of magnitude smaller than the precision presently attributed to the band-structure calculation. A more precise discussion of this point can be found in Ref. 6.

It had been pointed out in Ref. 9 that local-field effects

TABLE I. Band-structure energies of germanium for some selected high-symmetry points in units of eV. The energies are listed for the valence bands and four lowest conduction bands. All energies refer to the top of the spin-orbit-split valence band. The xc self-energy for the $\Gamma_{25'}$ state on the absolute scale is -0.13 eV. The spin-orbit coupling raises the top of the valence band by about 0.10 eV (Ref. 12). This has been taken into account for the LDA energies. The xc corrections $\Delta\Sigma^{xc}$ to be added to the LDA energies are given in column 1. The LDA values are taken from Refs. 11 and 12 (values in parentheses). The quasiparticle energies determined in the present work (column 3) are compared to those of Ref. 9 (column 4). The last column contains the experimental results from Refs. 38–41. If two experimental values are given they refer to spin-orbit-split bands. The present work yields correctly that the minimum gap is that from Γ to L of about 0.7–0.8 eV.

	$\Delta\Sigma^{xc}$	LDA	GWA	GWA (HL)	Expt.
$L_{2'}^c$	+ 0.16	+ 6.94 (+7.74)	+ 7.10 (+7.90)	+ 7.61	+ 7.81(1) ^a
L_3^c	+ 0.81	+ 3.64 (+3.63)	+ 4.45 (+4.44)	+ 4.33	+ 4.3(2) ^{b,a}
L_1^c	+ 0.73	+ 0.09 (−0.06)	+ 0.82 (+0.67)	+ 0.75	+ 0.744
$L_{3'}^v$	−0.04	−1.48	−1.43	−1.43	−1.4(3)
L_1^v	−0.33	−7.66	−7.99	−7.82	−7.7(2)
$L_{2'}^v$	−0.32	−10.72	−10.40	−10.89	−10.6(5)
Γ_{15}^c	+ 0.85	+ 2.47	+ 3.32	+ 3.26	+ 3.01,3.21
$\Gamma_{2'}^c$	+ 1.02	+ 0.00	+ 1.02	+ 0.71	+ 0.89 ^c
$\Gamma_{25'}^v$	+ 0.00	+ 0.00	+ 0.00	+ 0.00	+ 0.0
Γ_1^v	−0.36	−12.80	−13.16	−12.86	−12.9(2) ^d
X_3^c	+ 1.06	+ 9.36	+ 10.42		
X_1^c	+ 0.55	+ 0.60	+ 1.15	+ 1.23	+ 1.3(2)
X_4^v	−0.15	−3.15	−3.30	−3.22	−3.2(2)
X_1^v	−0.37	−8.74	−9.11	−9.13	−9.3(2) ^d

^aReference 41.

^bReference 38.

^cReference 40.

^dReference 39.

(the off-diagonal elements of the dielectric matrix) strongly influence the self-energy. These authors discussed that question in the framework of the static Coulomb-hole–screened-exchange (COHSEX) approximation introduced by Hedin.¹⁰ The local-field effects are indeed essential but not as important as the COHSEX approximation suggests. In the static approximation the huge Coulomb-hole term contributes only via the off-diagonal elements to the gap, while in the complete dynamic calculation the diagonal elements also contribute to it. The main effect of the local fields is a rigid shift of the valence band. Neglecting the off-diagonal elements from the very beginning leads to an almost rigid upwards shift of all valence-band states by about 0.4 eV relative to the conduction bands.

The results of our calculations are also in very close agreement with the results published earlier by Hybertsen and Louie.⁹ The only somewhat larger discrepancy occurs for the $\Gamma_{2'}$ state. Therefore these calculations and the work of Godby *et al.*⁵ suggest the *GW* approximation to be a promising method to perform precise and fast⁴² band-structure calculations for semiconductors and insulators.

VII. SUMMARY

In the present work we calculated the nonlocal and energy-dependent exchange-correlation self-energy using the *GW* approximation suggested by Hedin.¹⁰ The local approximation to the xc self-energy as used in the LDA is

calculated in addition. The difference of these two quantities defines the corrections to the LDA band structure and hence the quasiparticle energies.

Particular emphasis is put on the detailed discussion of the state dependence of the different contributions to the nonlocal xc self-energy. First, there is a global state dependence which is already present in the homogeneous electron gas. It is this state dependence that leads in semiconductors to appreciable corrections to the energy gap between valence and conduction bands. Secondly, there are fluctuations in the xc self-energy arising from the pronounced changes in the wave functions even within the same band.

In view of the quasiparticle equation (1) the Kohn-Sham equation can be interpreted as an approximate scheme for the calculation of band structures that omits essential parts of the nonlocal and energy-dependent self-energy. This is the source of the severe underestimate of energy gaps in LDA. An interesting point is the observation that the fluctuations appearing in the nonlocal exchange self-energy, which arise from anisotropy effects, the different symmetry of the wave functions, and their different localization within the unit cell, are rather well described by the LDA. There are, however, exceptions for those states which have a high amplitude in interstitial regions.

Nevertheless the remaining fluctuations in $\Delta\Sigma^{xc}$ invalidate the scissors operator concept. These fluctuations lead in Ge to relative shifts of about 0.3 eV for the different conduction-band states close to the gap. Hence

they are crucial for the physical conclusions, i.e., whether theory tells us that Ge is a direct- or an indirect-gap semiconductor.

The self-energy equations must be solved self-consistently, leading to the quasiparticle energies and wave functions. A convenient starting set is given by the DFT which in principle leads to the exact ground-state density. Hybertsen and Louie⁹ pointed out that the quasiparticle wave functions are almost identical to the wave functions obtained by the LDA. We have developed here a closed expression which allows the perturbative calculation of the quasiparticle wave functions and energies. This provides a tool for the study of the subtle differences between LDA, Hartree-Fock, and quasiparticle wave functions.

As a by-product we calculate the unscreened or exchange-only bands. For germanium considered here they are found to be in favorable agreement with the very recent and only other HF band-structure calculation of Ref. 17. A precise exchange-only calculation is a necessary prerequisite for the accuracy of the final quasiparticle band structure.

For the evaluation of the self-energy the dielectric matrix is a key quantity. The straightforward computation of it, even in the RPA, is rather time consuming. We developed a generalized plasmon-pole ansatz starting from the dielectric band structure, or in other words, the diagonal representation of the dielectric matrix. This ansatz fulfills the Johnson sum rule as well as the Kramers-Kronig relation and it leads to the correct analytic properties for all matrix elements. It turns out that this ansatz gives a fairly realistic description of the frequency dependence also for the off-diagonal elements which can generally not be characterized by a single-pole structure. This point will be discussed in more detail in a further paper.

A decisive point in these computations is the use of the plane-wave basis which makes the accurate evaluation of the GWA finally possible, as the matrix elements are conceivably simple. But it should not be concealed that a variety of systems exists for which plane waves are not an appropriate basis set. Among these is a great number of interesting substances, e.g., the transition metals and 4f systems. It is therefore a challenging task to develop an efficient program for the GWA in a mixed basis.

There are several very interesting open problems that can immediately be attacked with the GWA: (a) Energies and wave functions for impurity states, (b) conduction-band offsets in heterostructures or superlattices, (c) pressure dependence of band structures and thereby induced insulator-metal transitions, and (d) applications to low-symmetry systems. This list of interesting questions, which can very likely be answered with the GWA, can be easily continued.

The reason for the unexpectedly good results of the GWA is more or less an open issue. To clarify that point we are presently investigating the lowest-order vertex corrections. It has to be expected that these energies vary on a scale much larger than the Fermi energy, which is intuitively clear as vertex corrections describe the physics over short distances in real space.

ACKNOWLEDGMENTS

We would like to thank N. E. Christensen, O. Gunnarsson, L. Sham, and M. Schlüter for discussions and for the communication of results prior to publication. We are indebted to O. Jepsen and O. K. Andersen for providing us with the LMTO program. We are particularly grateful to P. Fulde for discussions and his encouragement of this line of work.

APPENDIX A: PERTURBATION THEORY FOR THE QUASIPARTICLE WAVE FUNCTIONS AND ENERGIES

In this appendix we outline the derivation of the expressions for the exact quasiparticle wave functions and energies given in Eq. (8). First the Hamiltonian is split into the Kohn-Sham Hamiltonian and the residue:

$$H = H_0(\{\rho(\mathbf{x})\}) + \Delta\Sigma^{xc}(\{\rho(\mathbf{x})\};\omega), \quad (\text{A1})$$

with the residual self-energy

$$\Delta\Sigma^{xc}(\{\rho(\mathbf{x})\};\omega) = \Sigma^{xc}(\{\rho(\mathbf{x})\};\omega) - \Sigma_{\text{KS}}^{xc}(\{\rho(\mathbf{x})\}). \quad (\text{A2})$$

Both parts of the Hamiltonian are functionals of the ground-state density. The following derivation is based on the assumption that the exact ground-state density is also used for H_0 . As a matter of fact, the Kohn-Sham Hamiltonian yields the exact density. Had we chosen another zeroth-order Hamiltonian the whole scheme would have to be performed iteratively with an improved density for H_0 at every cycle. The quasiparticle equation,

$$(\varepsilon_\mu - H_0) |\Phi_\mu\rangle = \Delta\Sigma(\varepsilon_\mu) |\Phi_\mu\rangle, \quad (\text{A3})$$

can be rewritten using the zeroth-order Green's function,

$$G_0(\omega) = \frac{1}{\omega - H_0(\{\rho^{\text{ex}}(\mathbf{x})\})}, \quad (\text{A4})$$

into the form

$$|\Phi_\mu\rangle = G_0(\varepsilon_\mu) \Delta\Sigma(\varepsilon_\mu) |\Phi_\mu\rangle, \quad (\text{A5})$$

where the energy argument in the Green's function has to be the exact quasiparticle energy. In the following we restrict the discussion to nondegenerate states. In general the results are the same for degenerate states as the xc corrections do not alter the degeneracy; otherwise a generalization is straightforward. Analogous to Eq. (A1) we split the wave function into the eigenstate of H_0 and an orthogonal correction:

$$\begin{aligned} |\Phi_\mu\rangle &= |\Phi_\mu^0\rangle + |\Phi_\mu^1\rangle, \\ \langle \Phi_\mu^0 | \Phi_\nu^0 \rangle &= \delta_{\mu\nu}, \\ \langle \Phi_\mu^0 | \Phi_\mu^1 \rangle &= 0. \end{aligned} \quad (\text{A6})$$

One has to be aware of the fact that the $|\Phi_\mu\rangle$ are not normalized. For convenient bookkeeping we introduce a projection operator P_μ projecting onto the space orthogonal to $|\Phi_\mu^0\rangle$:

$$P_\mu = (\mathbf{1} - |\Phi_\mu^0\rangle\langle\Phi_\mu^0|). \quad (\text{A7})$$

Applying P_μ on Eq. (A5) and allowing for Eqs. (A6) and (A7) leads to the following equivalent expressions for the exact quasiparticle wave functions:

$$\begin{aligned} |\Phi_\mu\rangle &= \frac{1}{\mathbf{1} - P_\mu G_0(\varepsilon_\mu)\Delta\Sigma(\varepsilon_\mu)} |\Phi_\mu^0\rangle, \\ |\Phi_\mu\rangle &= |\Phi_\mu^0\rangle + P_\mu G_0(\varepsilon_\mu)\Delta\Sigma(\varepsilon_\mu) |\Phi_\mu\rangle. \end{aligned} \quad (\text{A8})$$

The second relation embodies the generalized Dyson equation for the wave functions. To obtain the energy we multiply Eq. (A3) with $\langle\Phi_\mu^0|$. The resulting correction to the quasiparticle energy is

$$\Delta\varepsilon_\mu = \langle\Phi_\mu^0| \Delta\Sigma(\varepsilon_\mu) |\Phi_\mu\rangle. \quad (\text{A9})$$

In the derivation of this formula use has been made of

Eq. (A6).

Several points should be emphasized:

(i) The zeroth-order Green's function contains the exact ground-state density.

(ii) The energy argument of G_0 is the exact quasiparticle energy.

(iii) In contrast to the Lippmann-Schwinger formula a projection operator has to be taken into account.

The energy change given by Eq. (A9) shows that corrections to the first-order term $\langle\Phi_\mu^0| \Delta\Sigma |\Phi_\mu^0\rangle$ originate from the higher-order corrections to the DFT wave functions. These changes are believed to be small.

APPENDIX B: GENERALIZED f -SUM RULE

The Hermitian *causal* dielectric matrix⁴³ can be expressed by

$$\varepsilon_{\mathbf{G},\mathbf{G}'}^{-1}(\mathbf{q};\omega) - \delta_{\mathbf{G},\mathbf{G}'} = \frac{-8\pi}{V\|\mathbf{q}+\mathbf{G}\|\|\mathbf{q}+\mathbf{G}'\|} \sum_n \omega_{n0} \frac{\rho_{n0}(\mathbf{q}+\mathbf{G})\rho_{n0}^*(\mathbf{q}+\mathbf{G}')}{\omega^2 - (\omega_{n0} - i\delta)^2}. \quad (\text{B1})$$

With $\rho_{n0}(\mathbf{p}) = \langle 0 | e^{i\mathbf{p}\cdot\mathbf{x}} | n \rangle$ and $\omega_{n0} = E_n - E_0$ in terms of the exact many-body states $|n\rangle$ and energies E_n . Hence the generalization of the f -sum rule can be formulated as

$$\int_{-\infty}^{+\infty} \frac{d\omega}{2\pi i} \omega (\varepsilon_{\mathbf{G},\mathbf{G}'}^{-1}(\mathbf{q};\omega) - \delta_{\mathbf{G},\mathbf{G}'}) = \frac{-4\pi \langle 0 | [e^{i(\mathbf{q}+\mathbf{G})\cdot\mathbf{x}}, H] e^{-i(\mathbf{q}+\mathbf{G}')\cdot\mathbf{x}} | 0 \rangle}{V\|\mathbf{q}+\mathbf{G}\|\|\mathbf{q}+\mathbf{G}'\|} = -\frac{\omega_{\text{pl}}^2}{2} \frac{(\mathbf{q}+\mathbf{G})\cdot(\mathbf{q}+\mathbf{G}')}{\|\mathbf{q}+\mathbf{G}\|\|\mathbf{q}+\mathbf{G}'\|} \frac{\rho(\mathbf{G}-\mathbf{G}')}{\rho(\mathbf{0})}. \quad (\text{B2})$$

Here $\omega_{\text{pl}}^2 = 4\pi\rho(\mathbf{0})$ is the free-electron plasma frequency. For the derivation of Eq. (B2) use has been made of the fact that the ground state is an eigenstate of the momentum operator with eigenvalue equal to zero. Furthermore as the potential part of the Hamiltonian commutes with $e^{i(\mathbf{q}+\mathbf{G})\cdot\mathbf{x}}$ only the comutator with H_{kin} has to be evaluated, which is an easy task.

The advantage of the expression in Eq. (B2) is that it reveals how the f -sum rule changes with a basis transformation $U_{q,i}(\bar{\mathbf{G}})$:

$$\begin{aligned} \int_{-\infty}^{+\infty} \frac{d\omega}{2\pi i} \omega (\varepsilon_{i,j}^{-1}(\mathbf{q};\omega) - \delta_{i,j}) &= -\frac{\omega_{\text{pl}}^2}{2} \sum_{\mathbf{G},\mathbf{G}'} U_{\bar{q},i}^*(\bar{\mathbf{G}}) \frac{(\mathbf{q}+\mathbf{G})\cdot(\mathbf{q}+\mathbf{G}')}{\|\mathbf{q}+\mathbf{G}\|\|\mathbf{q}+\mathbf{G}'\|} \frac{\rho(\mathbf{G}-\mathbf{G}')}{\rho(\mathbf{0})} U_{q,j}(\bar{\mathbf{G}}') \\ &= -\frac{\omega_{\text{pl}}^2}{2\rho(\mathbf{0})} \int d^3x \rho(\mathbf{x}) [\nabla_{\mathbf{x}}\Psi_{q,i}(\mathbf{x})] \cdot [\nabla_{\mathbf{x}}\Psi_{q,j}(\mathbf{x})]^*, \end{aligned} \quad (\text{B3})$$

with the real-space eigenpotentials defined as

$$\Psi_{q,i}(\mathbf{x}) = \sum_{\mathbf{G}} \frac{U_{\bar{q},i}(\bar{\mathbf{G}}) e^{-i(\mathbf{q}+\mathbf{G})\cdot\mathbf{x}}}{\|\mathbf{q}+\mathbf{G}\|}. \quad (\text{B4})$$

APPENDIX C: BRILLOUIN-ZONE INTEGRALS WITH SINGULAR INTEGRANDS

The numerical evaluation of Brillouin-zone integrals of the form

$$\int_{\text{BZ}} d^3k \frac{f(\mathbf{k})}{\|\mathbf{k}-\mathbf{k}_0\|^2} \quad (\text{C1})$$

entering the expression for the self-energy causes some trouble due to the singular denominator. To circumvent this problem the authors of Refs. 5, 9, 15, and 17 used the midpoint rule, thereby replacing the singular terms by

the spherical average.

We have chosen the following procedure. Due to the singularity of the integrand the latter has to be computed for a large number of integration points. On the other hand $f(\mathbf{k})$ is not known analytically and its numerical computation is quite time consuming. The problem can be eluded by making use of the fact that $f(\mathbf{k})$ is well behaved and therefore can be interpolated by simple functions. This leads to analytic expressions for the integrand which can be evaluated for any number of integration points.

To begin with we divide the whole integration volume

into N equal reduced copies ΔV of it, which have their centers at points \mathbf{k}_i :

$$\int_{\text{BZ}} d^3k \frac{f(\mathbf{k})}{\|\mathbf{k}-\mathbf{k}_0\|^2} = \sum_{i=1}^N \int_{\Delta V} d^3k \frac{f(\mathbf{k}+\mathbf{k}_i)}{\|\mathbf{k}+\mathbf{k}_i-\mathbf{k}_0\|^2}. \quad (\text{C2})$$

As $f(\mathbf{k}+\mathbf{k}_i)$ is a smooth function we can expand it into a Taylor series around the point \mathbf{k}_i .

As a matter of fact the linear term in \mathbf{k} is of the same order as the quadratic one, namely of order $O(h^2)$, where h is the diameter of ΔV . Therefore the first term in the Taylor expansion already leads to a quadratic scheme:

$$\int_{\text{BZ}} d^3k \frac{f(\mathbf{k})}{\|\mathbf{k}-\mathbf{k}_0\|^2} = \sum_{i=1}^N f(\mathbf{k}_i) \int_{\Delta V} d^3k \frac{1}{\|\mathbf{k}+\mathbf{k}_i-\mathbf{k}_0\|^2}. \quad (\text{C3})$$

The remaining integrals are performed numerically with high accuracy. To obtain an accuracy of $O(0.001 \text{ eV})$ it is

sufficient to take $N=343$ equidistant points \mathbf{k}_i corresponding to 20 points in the irreducible part of the Brillouin zone.

The simple midpoint rule leads, in the case of the HFA band structure, to an underestimate of the direct gap of germanium by 0.3 eV. This underestimate has also been noted by Gygi and Baldereschi.¹⁶ They pointed out that the midpoint rule used by Ohkoshi¹⁵ in a calculation of the HF band structure of silicon tends to underestimate the gap by about 1 eV as compared to their integration scheme. For Si we find a somewhat smaller discrepancy of 0.5 eV. Nevertheless that is a significant contribution as far as the HFA results are concerned. In covalent semiconductors, however, the error in the final exchange-correlation energies is reduced to about 0.01 eV and can be neglected. Hence the more accurate treatment of the Brillouin-zone integrals becomes more important for wide-gap semiconductors or insulators.

- ¹P. Hohenberg and W. Kohn, Phys. Rev. **136**, B864 (1964).
²W. Kohn and L. J. Sham, Phys. Rev. **140**, A1133 (1965).
³J. P. Perdew and M. Levy, Phys. Rev. Lett. **51**, 1884 (1983).
⁴L. J. Sham and M. Schlüter, Phys. Rev. Lett. **51**, 1888 (1983).
⁵R. W. Godby, M. Schlüter, and L. J. Sham, Phys. Rev. Lett. **56**, 2415 (1986); Phys. Rev. B **35**, 4170 (1987).
⁶W. v. d. Linden, P. Horsch, and W. D. Lukas, Solid State Commun. **59**, 485 (1986).
⁷W. Kohn, Rev. B **33**, 4331 (1986).
⁸S. Horsch, P. Horsch, and P. Fulde, Phys. Rev. B **28**, 5977 (1983); **29**, 1870 (1984).
⁹M. S. Hybertsen and S. G. Louie, Phys. Rev. B **34**, 5390 (1986); Phys. Rev. Lett. **55**, 1418 (1985).
¹⁰L. Hedin, Phys. Rev. **139**, A796 (1965). For a review, see L. Hedin and S. Lundqvist, in *Solid State Physics: Advances in Research and Applications*, edited by F. Seitz, D. Turnbull, and H. Ehrenreich (Academic, New York, 1969), Vol. 23, p. 1.
¹¹G. B. Bachelet and N. E. Christensen, Phys. Rev. B **31**, 879 (1985), and references therein.
¹²N. E. Christensen (private communication).
¹³R. Dovesi, C. Pisani, F. Ricca, and C. Roetti, Phys. Rev. B **22**, 5936 (1980).
¹⁴W. v. d. Linden, P. Fulde, and K. P. Bohnen, Phys. Rev. B **34**, 1063 (1986), and references therein.
¹⁵I. Ohkoshi, J. Phys. C **18**, 5415 (1985).
¹⁶F. Gygi and A. Baldereschi, Phys. Rev. B **34**, 4405 (1986).
¹⁷A. Svane, Phys. Rev. B **35**, 5496 (1987).
¹⁸G. Strinati, H. J. Mattausch, and W. Hanke, Phys. Rev. B **25**, 2867 (1982).
¹⁹A. Baldereschi and E. Tosatti, Solid State Commun. **20**, 131 (1979).
²⁰P. Minnhagen, J. Phys. C **7**, 3013 (1974).
²¹K. Schönhammer and O. Gunnarsson, Phys. Rev. Lett. **56**, 1968 (1986); J. Phys. C **20**, 3675 (1987).
²²The result of Ref. 4 was obtained to first order in the change of the unperturbed Green's function. The higher-order analysis leads to corrections corresponding to the effect of a projection operator [L. Sham (private communication)].
²³S. L. Adler, Phys. Rev. **126**, 413 (1962); N. Wiser, *ibid.* **129**, 62 (1963).
²⁴A. Baldereschi and E. Tosatti, Phys. Rev. B **17**, 4710 (1978).
²⁵R. Resta and A. Baldereschi, Phys. Rev. B **23**, 6615 (1981).
²⁶D. J. Chadi and M. L. Cohen, Phys. Rev. B **8**, 5747 (1973).
²⁷R. Car, E. Tosatti, S. Baroni, and S. Leelaprute, Phys. Rev. B **24**, 985 (1981).
²⁸In the scheme of Ref. 9 every matrix element of the DM is represented by a one-pole function. The single-pole ansatz leads for certain off-diagonal elements to an imaginary plasmon frequency and to negative pole strength. Because these terms appear to have very little weight, they have been discarded in Ref. 9.
²⁹J. C. Phillips, Phys. Rev. **125**, 1931 (1962).
³⁰D. Brust, Phys. Rev. **133**, A1337 (1964).
³¹M. Cohen and T. K. Bergstresser, Phys. Rev. **141**, 789 (1966).
³²W. Saslow, T. K. Bergstresser, and M. Cohen, Phys. Rev. Lett. **16**, 354 (1966).
³³V. Heine and R. O. Jones, J. Phys. C **2**, 719 (1969).
³⁴H. W. A. M. Rompa, M. F. H. Schuurmans, and F. Williams, Phys. Rev. Lett. **52**, 675 (1984).
³⁵A. Svane and O. K. Andersen, Phys. Rev. B **34**, 5512 (1986).
³⁶O. K. Andersen and O. Jepsen, Phys. Rev. Lett. **53**, 2571 (1984).
³⁷P. Horsch, Solid State Commun. **54**, 741 (1985).
³⁸Landolt-Börnstein, *Zahlenwerte und Funktionen aus Naturwissenschaft und Technik* (Springer-Verlag, New York, 1982), Vol. III, pt. 17a.
³⁹A. L. Wachs *et al.*, Phys. Rev. B **32**, 2326 (1985).
⁴⁰D. E. Aspnes, Phys. Rev. B **12**, 2797 (1975).
⁴¹D. Straub, L. Ley, and F. J. Himpsel, Bull. Am. Phys. Soc. **30**, 559 (1985).
⁴²The fastest version of our band-structure program requires about 20 min on a Cray-XMP computer. This version uses a model for the static dielectric matrix [P. Horsch and W. von der Linden (unpublished)]. Otherwise the computation time amounts to several hours.
⁴³P. Ziesche and G. Lehmann, *Elektronentheorie der Metalle* (Springer-Verlag, Berlin, 1983), pp. 249ff. We used the *time-ordered* dielectric function. The only difference lies in the signs of the infinitesimal shifts into the imaginary plane.